Line-Strength Indices in Bright Spheroidals: Evidence for a Stellar Population Dichotomy between Spheroidal and Elliptical Galaxies

Javier Gorgas[1], Santos Pedraz[1], Rafael Guzmán[2], Nicolás Cardiel[1], J. Jesús González[3]

Received ______________________; accepted ______________________

[1]Departamento de Astrofísica, Facultad de Físicas, Universidad Complutense, Madrid, E28040, Spain.

[2]UCO/Lick Observatory, University of California, Santa Cruz, CA 95064.

[3]Instituto de Astronomía, U.N.A.M., Apdo. Postal 70–264, 04510 Mexico D.F., Mexico

ABSTRACT

We present new measurements of central line-strength indices (namely Mg_2, $\langle Fe \rangle$, and $H\beta$) and gradients for a sample of 6 bright spheroidal galaxies (Sph's) in the Virgo cluster. Comparison with similar measurements for elliptical galaxies (E's), galactic globular clusters (GGC's), and stellar population models yield the following results: (1) In contrast with bright E's, bright Sph's are consistent with solar abundance [Mg/Fe] ratios; (2) Bright Sph's exhibit metallicities ranging from values typical for metal-rich GGC's to those for E's; (3) Although absolute mean ages are quite model dependent, we find evidence that the stellar populations of some (if not all) Sph's look significantly younger than GGC's; and (4) Mg_2 gradients of bright Sph's are significantly shallower than those of E galaxies. We conclude that the dichotomy found in the structural properties of Sph and E galaxies is also observed in their stellar populations. A tentative interpretation in terms of differences in star formation histories is suggested.

Subject headings: galaxies: evolution — galaxies: abundances — galaxies: stellar content

1. Introduction

Over the last few years it has been established the existence of a structural dichotomy between elliptical (E) and spheroidal (Sph) galaxies[4] (see e.g. Kormendy 1985 and Binggeli & Cameron 1991) which suggests different galaxy formation/evolution processes for both kind of galaxies (Dekel & Silk 1986; Guzmán, Lucey & Bower 1993). However, this dichotomy contrasts with the remarkable similarity in the global properties of their stellar populations. In particular, the colour-luminosity relation as well as the correlation between the Mg_2 line-strength index and velocity dispersion are apparently universal for both galaxy families (Caldwell 1983; Bender 1991). A detailed comparison of the star-formation histories of Sph's and E's is required to provide constraints on their formation mechanisms. Also, understanding the star-formation history of Sph's is of vital importance for cosmological issues such as the nature of the faint blue galaxies (Babul & Rees 1992) or the faint end of the luminosity function.

Recent studies devoted to compare in detail the stellar populations of Sph's and E's have led to ambiguous results so far. For dwarf Sph's in the Local Group, there is now clear evidence of recent (i.e., 3-5 Gyrs) star-forming events (see e.g. da Costa 1991). Spectroscopic studies have provided evidence that some bright Sph's do exhibit a young or intermediate age stellar population (Gregg 1991; Held & Mould 1994). However, the general trend is that bright Sph's tend to follow the galactic globular clusters (GGC's) locus in the color–line-strength diagrams, but with a large scatter (Bothun & Mould 1988; Brodie & Huchra 1991; Held & Mould 1994). Ferguson (1994) has compared colors and line-strengths for Sph's, E's and GGC's with the predictions of stellar population models, concluding that

[4]Throughout this *Letter* we adopt the nomenclature of Kormendy & Bender (1994), i.e. low-density, dwarf ellipsoidal galaxies like NGC 205 are called 'spheroidals', instead of that of Binggeli (1994), in which these galaxies are named 'dwarf ellipticals'.

differences in the line-strength–color relations may arise due to calibration problems and the relatively large uncertainties in both the measurements and the population synthesis models. Clearly, a systematic study with more precise measurements is needed to derive any serious constraints on the stellar populations of Sph galaxies. In this *Letter* we show the first results of a spectroscopic survey of Sph's aimed at studying in detail their stellar populations and kinematics. The analysis presented here is based on new central measurements of line-strength indices (namely Mg_2, Fe5270, Fe5335, and Hβ) and, for the first time, gradients for a sample of six Sph's in the Virgo cluster.

2. The data

The galaxy sample listed in Table 1 includes six bright Sph's in the Virgo cluster. Long-slit spectroscopic observations were carried out during April 11-15 1994, with the 2.5m INT at La Palma. The IDS spectrograph provided 2.5 Å(FWHM) resolution spectra in the wavelength range 4700–6100 Å . The slit was aligned with the major axis. Exposure times (typically $\sim$4 hours per galaxy) allow measurements of spectral features out to the galaxy effective radius r_e. Spectra of the central regions have very high quality (the signal-to-noise ratio ranges from 32 to 110). A detailed description of the observational setup and reduction procedures will be given in Gorgas et al. (1997). We emphasize that, in order to ensure reliable line-strength gradients, the sky was carefully estimated at the slit ends taking into account any possible contribution of the galaxy itself and the effect of scattered light. For each galaxy spectrum we measured the Mg_2, Hβ, Fe5270, and Fe5335 indices. The errors in these measurements were estimated by reducing, in parallel to the galaxy frames, error images created from photon and readout noises. Since line-strength indices depend on spectral resolution, our spectra were broadened to match the resolution of the widely used Lick system (200 km s^{-1}). To ensure the accuracy of this correction and

check for any systematic errors, we observed a sample of 39 F–M stars from the Lick stellar library (Gorgas et al. 1993). After the broadening correction, we found no systematic deviations for the Fe and Hβ indices between both data sets. The Mg_2 index, however, shows a systematic offset of 0.013 magnitudes (our values below those of Lick), which was applied to convert our indices to the Lick system.

3. Central line-strength indices

In Table 1 we list, for our galaxy sample, the central Mg_2, Hβ and $\langle$Fe$\rangle$ line-strength indices, and their formal errors in a $2'' \times 4''$ aperture centered on the galaxy nucleus. In Figure 1 we present line-strength diagrams for our sample of Sph's as well as for a representative sample of GGC's and E galaxies. We also show the predictions of single-burst stellar population models of a given age and metallicity (Worthey 1994). It is immediately apparent that, in the Mg_2–$\langle$Fe$\rangle$ plane, bright Sph's do not follow the extrapolation of the E sequence towards lower Mg_2 values, but tend to resemble metal-rich GGC's.

The failure to reproduce theoretically the high Mg_2 values observed in bright E's has been interpreted to be due to an enhancement of the [Mg/Fe] ratio in these galaxies relative to the solar ratio assumed in the population models (Peletier 1989; Worthey, Faber, & González 1992; Davies, Sadler & Peletier 1993, hereafter DSP). From Fig. 1a, it is clear that the model lines pass through the Sph's locus thus suggesting solar abundance [Mg/Fe] ratios for these galaxies. This difference in [Mg/Fe] between E's and Sph's may likely imply different star-formation histories for both galaxy types. If the enhancement of [Mg/Fe] is due to an overabundance of light elements in bright E's, then it is plausible that the star-formation in these galaxies occurred in a short timescale, since Mg is created rapidly by Type II SNs whilst Fe is produced in a longer timescale by Type Ia SNs. Under this assumption, our observations imply a longer star-formation period in Sph's as compared

to E's. In other words, the star-forming event should have elapsed long enough to yield a solar [Mg/Fe] ratio. However, other factors, such as a flatter IMF in giant E's compared to Sph's, could account for the Mg overabundance difference (Worthey et al. 1992).

The positions of the bright Sph's in the $\langle \mathrm{Fe} \rangle$– H$\beta$ diagram also reveal a clear dichotomy in the way Sph's and E's populate the age-metallicity plane (Fig. 1b). Comparison between the measured indices and the spectral synthesis models in this diagram allow us to break the degeneracy between age and metallicity present in Fig. 1a. Within the errors, bright Sph's exhibit a large range of metallicities, from values typical for metal rich GGC's ([Fe/H]~ -0.75) to those for E's. We note that the derived metallicities for Sph's are the same, and lower than for E's, whether computed from Mg or Fe lines.

Concerning the age question, we find that bright Sph's span a wide range in mean stellar ages, showing in fact a comparable age spread to that derived, using a similar diagram, by González (1993, hereafter G93) for E galaxies. Most interestingly, we find a trend between age and metallicity, in the sense that "younger" Sph's tend to be more metal-rich, although the sample is too small to reach a firm conclusion. It is important to note that the computed ages are light-weighted mean stellar ages. Moreover, since single burst models are probably a naive approximation to the star forming history of early-type galaxies, and given the discrepancies in the derived ages when using different models (typically ~ 4 Gyrs for old populations and metallicities around solar; cf. Worthey 1994; Vazdekis et al. 1996; see Fig 1b), it is hard to give any reliable estimate of absolute ages, but the relative trends remain. Perhaps the key question is whether some Sph's (like UGC 7436 and NGC 4431) are as old as the oldest E's. Fig. 1b suggests that this is the case but this conclusion may be subject to other effects. Since the slope of the constant-age lines (for old stellar populations) in the $\langle \mathrm{Fe} \rangle$–H$\beta$ plane is not model dependent, it is hard to reconcile the relative positions of the low-Hβ E's and metal-rich GGC's in this diagram with

the idea that both are old and coeval. Vazdekis et al. (1996) have shown that the location of those constant-age lines depends on the adopted IMF slope (see Fig 1b). Therefore, the assumption of a flatter IMF for the bright E's would help to explain the position of both populations (GGC's and low-Hβ E's) in this diagram without introducing important age differences, accounting at the same time for the Mg overabundance effect. Under this view, the stellar populations of all bright Sph's of the sample (with solar Mg/Fe ratios) could be significantly younger than GGC's and, therefore, than the oldest bright E's.

An important question raised by Ferguson & Binggeli (1994) is whether the stellar populations of Sph's resemble those in the outer regions of E's. Using line-strength profiles from G93, when the comparison is made at constant surface brightness ($\mu_B = 20 - 21$ mag arcsec^{-2}, corresponding to the Sph mean brightness inside our central aperture), E galaxies attain typical Mg_2 line-strengths of ~ 0.28 mag, which are significantly larger than those observed for Sph's (see Table 1). Therefore, the stellar populations are, again, different and local surface brightness does not seem to be a main parameter in fixing the properties of the stellar populations, suggesting that local stellar populations mostly reflect the global properties (e.g. mass), and only secondarily the local environment.

4. Line-strength gradients

Radial profiles of Mg_2, $\langle Fe \rangle$ and Hβ for our galaxy sample are plotted in Figure 2. Each point along radius corresponds to an average of line-strengths from symmetrical bins at both sides of the galaxy. For the outer regions, we co-added a sufficient number of spectra in the spatial direction to guarantee a minimum signal-to-noise per Å, leading to typical errors outside the centers of $\Delta Mg_2 = 0.011$ mag, $\Delta\langle Fe \rangle = 0.24$ Å and $\Delta H\beta = 0.36$ Å. The gradients have been estimated from the error-weighted linear regression fits over the radial range covering from $1.5''$ (in order to avoid seeing effects) to the effective radius.

As it is apparent from Fig. 2, bright Sph's possess shallow Mg_2 gradients. The mean Mg_2 gradient ($\langle d\mathrm{Mg}_2/d\log r\rangle$) for our sample is -0.020, with a r.m.s. dispersion around the mean of 0.012. This value can be compared with the mean Mg_2 gradient derived by González & Gorgas (1997) using published and unpublished data for 109 early-type galaxies with reliable Mg_2 profiles. Following a fitting procedure similar to that described above, the derived mean Mg_2 gradient for E's is -0.055, with a scatter of 0.025. Applying the Mann–Whitney U-test, we conclude that Mg_2 gradients in bright Sph's are flatter than those in E galaxies at the 0.0005 level of confidence. Due to their dependence on spectral resolution and photon noise, Fe indices are worse determined than Mg_2. Nevertheless, Fe gradients in bright Sph's are also found to be moderately shallow. The mean $\langle \mathrm{Fe}\rangle$ gradient for the sample is -0.32 with a scatter of 0.23. Combining data from Gorgas, Efstathiou & Aragón-Salamanca (1990), DSP and G93 we have derived a mean $\langle \mathrm{Fe}\rangle$ gradient for a sample of 50 E's of -0.43 (with a scatter of 0.29). This is also steeper than the gradients in our sample of Sph's, although at a confidence level of only 0.26.

Concerning Hβ gradients, it is clear from Fig. 2 that almost all bright Sph's in our sample exhibit essentially flat gradients in the Hβ strength. Hβ line-strengths could be affected by filling due to weak nebular emission. It must be noted, however, that no [OIII] λ5007 Å emission lines are detectable in the spectra of these galaxies. For our sample, we derive $< d\mathrm{H}\beta/d\log r >= -0.11$, with a r.m.s scatter of 0.41, consistent with a flat mean gradient. This result agrees with what has been found for this feature in several samples of E galaxies (Gorgas et al. 1990; DSP; G93).

These line-strength gradients should be interpreted in terms of radial variations in mean age and metallicity. If we assumed that Mg_2 gradients are entirely due to metallicity variations within galaxies, then, using Worthey (1994) models, these gradients would translate into a mean $\langle \Delta[\mathrm{Fe/H}]/\Delta\log r\rangle = -0.14 \pm 0.04$, considerably flatter than the mean

metallicity gradient, derived in a similar way, for E's (−0.22, Gorgas et al. 1990; −0.23, DSP; −0.25, Fisher, Franx & Illingworth 1995). The constancy of Hβ along radius in galaxies with negative metallicity gradients has been interpreted, when taking the models literally, as an evidence for age gradients (G93; Fisher et al. 1995). This result would also apply to our sample of Sph's. Although there is a large variation from galaxy to galaxy, our data suggest moderate age gradients, in the sense of younger-looking stellar populations in the inner regions relative to the outer parts. Color gradients in Sph galaxies have previously been studied by Vader at al. (1988) and Chaboyer (1994). Their main conclusion is that Sph's exhibit shallower gradients than E's, being, in the mean, compatible with a flat B–R colour gradient. These results are fully consistent with our line-strength gradients since age and metallicity effects would tend to cancel to yield shallow color gradients. Note that, in the presence of age gradients, the above estimate for the mean metallicity gradient would be in fact underestimated (by ~ 0.10 dex). In any case, since this would also apply to giant E's, the metallicity gradients in Sph's still remain shallower than those in E galaxies. This result suggests that SN-driven winds, or other heating mechanism, governs the chemical evolution of Sph's, reducing the infall of enriched gas towards the galaxy centers and preventing, therefore, the development of steep metallicity gradients.

5. Conclusions

Through the study of absorption features, we present evidence that the dichotomy found between the structural properties of Sph's and E's (e.g. Bender, Burstein & Faber 1992) is also observed in the stellar populations. This dichotomy rests mainly upon the observed differences in Mg/Fe overabundance, global metallicity and metallicity gradients. Although, in the light of the available stellar population models, these results are still unable to identify unambiguously the differences in the star formation histories of the E and

Sph families, our suggestion is that, while the bulk of star formation in giant E's occurred in a short timescale and probably with a IMF skewed towards higher masses, star formation in Sph's has proceeded, self-regulated by galactic winds or other mechanisms, quietly in a longer timescale and with less amount of dissipation. Further work is needed to decide whether this elapsed star-forming period would be able to account for the young mean ages observed in some (if not all) Sph's or whether subsequent starbursts should be invoked. It is clear that other important aspects, like the possible differences between the stellar populations of nucleated and non-nucleated Sph's and the influence of environment, require further investigation before we can have a more complete picture of the star-formation history in spheroidal galaxies.

We are grateful to the anonymous referee, A. Aragón-Salamanca, J. Gallego and R. Peletier for useful comments. The INT is operated on the island of La Palma by the RGO at the Observatorio del Roque de los Muchachos of the Instituto de Astrofísica de Canarias. This work was supported in part by the Spanish grant No. PB93-456. R. G. acknowledges funding from the Spanish MEC fellowship EX93-27295297 and NSF grant AST91–20005.

REFERENCES

Babul, A., & Rees, M. 1992, MNRAS, 255, 346

Bender, R. 1991, in IAU Symp. 149, The Stellar Populations of Galaxies, ed. B. Barbuy & A. Renzini (Dordrecht: Kluwer), 269

Bender, R., Burstein, D., & Faber, S. M. 1992, ApJ, 399, 462

Binggeli, B. 1994, in Dwarf Galaxies, ESO Conf. and Workshop Proc. 49, ed. G. Meylan & P. Prugniel (Haute Provence: ESO), 13

Binggeli, B., & Cameron, L. M. 1991, A&A, 252, 27

Binggeli, B., Sandage, A., & Tammann, G. A. 1985, AJ, 90, 1681

Bothun, G. D., & Mould, J. R. 1988, ApJ, 324, 123

Brodie, J. P., & Huchra, J. P. 1991, ApJ, 379, 157

Burstein, D., Faber, S. M., Gaskell, C. M., & Krumm, N. 1984, ApJ, 287, 586

Caldwell, N. 1983, AJ, 88, 804

Covino, S., Galletti, S., & Pasinetti, L. E. 1995, A&A, 303, 79

Chaboyer, B. 1994, in Dwarf Galaxies, ESO Conf. and Workshop Proc. 49, ed. G. Meylan & P. Prugniel (Haute Provence: ESO), 485

da Costa, G. S. 1991, in IAU Symp. 149, The Stellar Populations of Galaxies, ed. B. Barbuy & A. Renzini (Dordrecht: Kluwer), 191

Davies, R. L., Sadler, E. M., & Peletier, R. F. 1993, MNRAS, 262, 650 (DSP)

Dekel, A., & Silk, J. 1986, ApJ, 303, 39

Ferguson, H. C. 1994, in Dwarf Galaxies, ESO Conf. and Workshop Proc. 49, ed. G. Meylan & P. Prugniel (Haute Provence: ESO), 475

Ferguson, H. C., & Binggeli, B. 1994, A&A Rev., 6, 67

Fisher, D., Franx, M., & Illingworth, G. 1995, ApJ, 448, 119

González, J. J. 1993, PhD Thesis, University of California, Santa Cruz (G93)

González, J. J., & Gorgas, J. 1997, in preparation.

Gorgas, J., Efstathiou, G., & Aragón-Salamanca, A. 1990, MNRAS, 245, 217

Gorgas, J., Faber, S. M., Burstein, D., González, J. J., Courteau, S., & Prosser, C. 1993, ApJS, 86, 153

Gorgas, J., Pedraz, S., Guzmán, R., González, J. J., & Cardiel, N. 1997, in preparation.

Gregg, M. D. 1991, in IAU Symp. 149, The Stellar Populations of Galaxies, ed. B. Barbuy & A. Renzini (Dordrecht: Kluwer), 426

Guzmán, R., Lucey, J. R., & Bower, R. G. 1993, MNRAS, 265, 731

Held, E. V., & Mould, J. R. 1994, AJ, 107, 1307

Kormendy, J. 1985, ApJ, 295, 73

Kormendy, J, & Bender, R. 1994, in Dwarf Galaxies, ESO Conf. and Workshop Proc. 49, ed. G. Meylan & P. Prugniel (Haute Provence: ESO), 161

Peletier, R. F. 1989, PhD Thesis, Rijksuniversiteit Groningen

Salpeter, E. E. 1955, ApJ, 121, 161

Vader, J. P., Vigroux, L., Lachièze-Rey, M., & Souviron, J. 1988, A&A, 203, 217

Vazdekis A., Casuso, E., Peletier, R. F., & Beckman, J. E. 1996, ApJS, 106, 307

Worthey, G. 1994, ApJS, 95, 107

Worthey, G., Faber, S. M., & González, J. J. 1992, ApJ, 398, 69

This manuscript was prepared with the AAS LaTeX macros v4.0.

Fig. 1.— Line-strength diagrams for GGC's (asterisks, from Burstein et al. 1984, and Covino, Galletti & Pasinetti 1995), E galaxies (open circles, from G93) and the central regions of bright Sph's (filled circles). Open triangles represent compact E's from G93 (M 32) and Gorgas et al. (1997) (NGC 5846A and IC 767). The straight line in panel (a) is a least-square fit to the G93 sample of E's. Predictions from stellar population models (Worthey 1994) are shown as dotted lines (for fixed ages of 1.5, 2, 3, 5, 8, 12 and 17 Gyr, from top to bottom in panel (b)) and dot-dashed lines (for fixed metallicities of [Fe/H]= $-2.0, -1.5, -1.0, -0.5, -0.25, 0.0, 0.25, 0.50$, from left to right in panel (b)). These lines overlap in panel (a). Full lines in (b) represent the predictions of single-burst models from Vazdekis et al. (1996) for a 17 Gyr old stellar population, metallicities [Fe/H] $= -0.4, 0, 0.4$ (from left to right), and different IMF slopes ($x = 1.35$ corresponds to Salpeter (1955) IMF and it is the slope used in Worthey models). The discrepancy between both sets of models is mainly due to differences in the temperatures of the adopted isochrones. Error bars show the typical observational errors in the indices of Sph's (large crosses) and E's (small crosses).

Fig. 2.— Mg_2, $\langle Fe \rangle$ and Hβ gradients for our sample of bright Sph's. Straight lines represent error-weighted least-squares fits to points between $1.5''$ and the effective radius (r_e). For each galaxy we give the derived gradients and their formal errors. The individual profiles have been shifted vertically by arbitrary amounts; tick marks on the ordinate axis correspond to 0.02 magnitudes for Mg_2, and 1 Å for the atomic indices ($\langle Fe \rangle$ and Hβ). The central indices listed in Table 1 correspond to the added spectra of the two innermost points in the line-strength profiles.

Table 1. Central line-strengths.

Galaxy	M_B[a]	σ[b]	Mg_2	Hβ	$\langle Fe \rangle$[c]
NGC 4415	-17.76	–	0.182±0.005	1.97±0.20	2.35±0.13
NGC 4431	-17.99	68	0.184±0.005	1.88±0.20	2.15±0.14
NGC 4489	-18.76	48	0.213±0.002	2.40±0.08	2.77±0.06
IC 794	-17.42	54	0.212±0.005	2.11±0.22	2.72±0.14
IC 3393	-17.07	55	0.142±0.006	2.16±0.25	2.13±0.17
UGC 7436	-17.27	45	0.157±0.006	1.90±0.27	1.88±0.18

[a]Sources for B_T are Binggeli et al. 1985 and Binggeli & Cameron 1991. A distance to Virgo of 20.7 Mpc has been adopted (Bender et al. 1992)

[b]Central velocity dispersion, in km s^{-1}, from Bender et al. 1992 and G93

[c]$\langle Fe \rangle$ is defined as $(Fe5270 + Fe5335)/2$

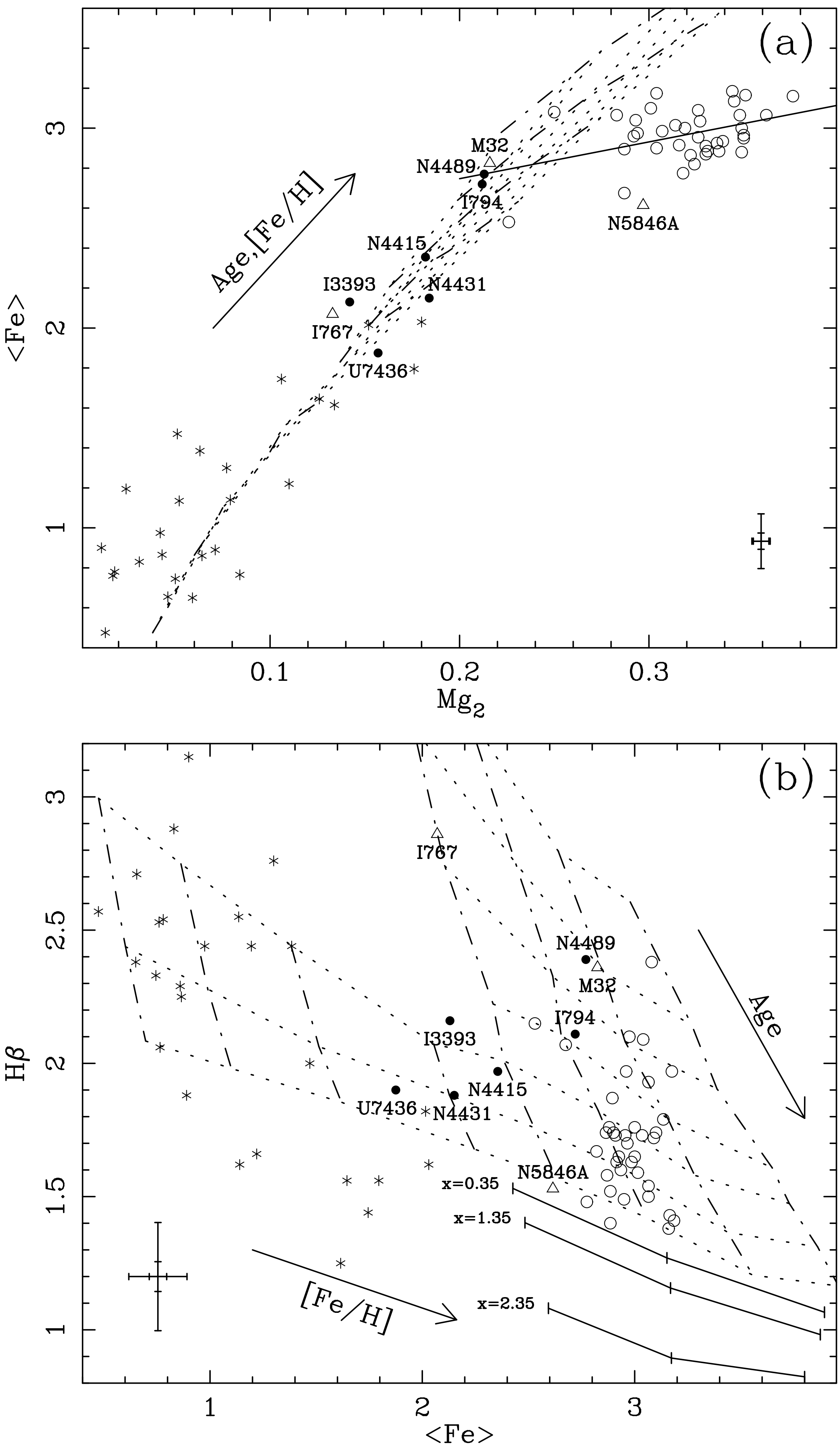

(a)
Age,[Fe/H]
M32
N4489
I794
N5846A
N4415
I3393
N4431
I767
U7436
<Fe>
Mg$_2$
(b)
I767
N4489
M32
I794
I3393
N4415
N4431
U7436
N5846A
Age
[Fe/H]
x=0.35
x=1.35
x=2.35
Hβ
<Fe>

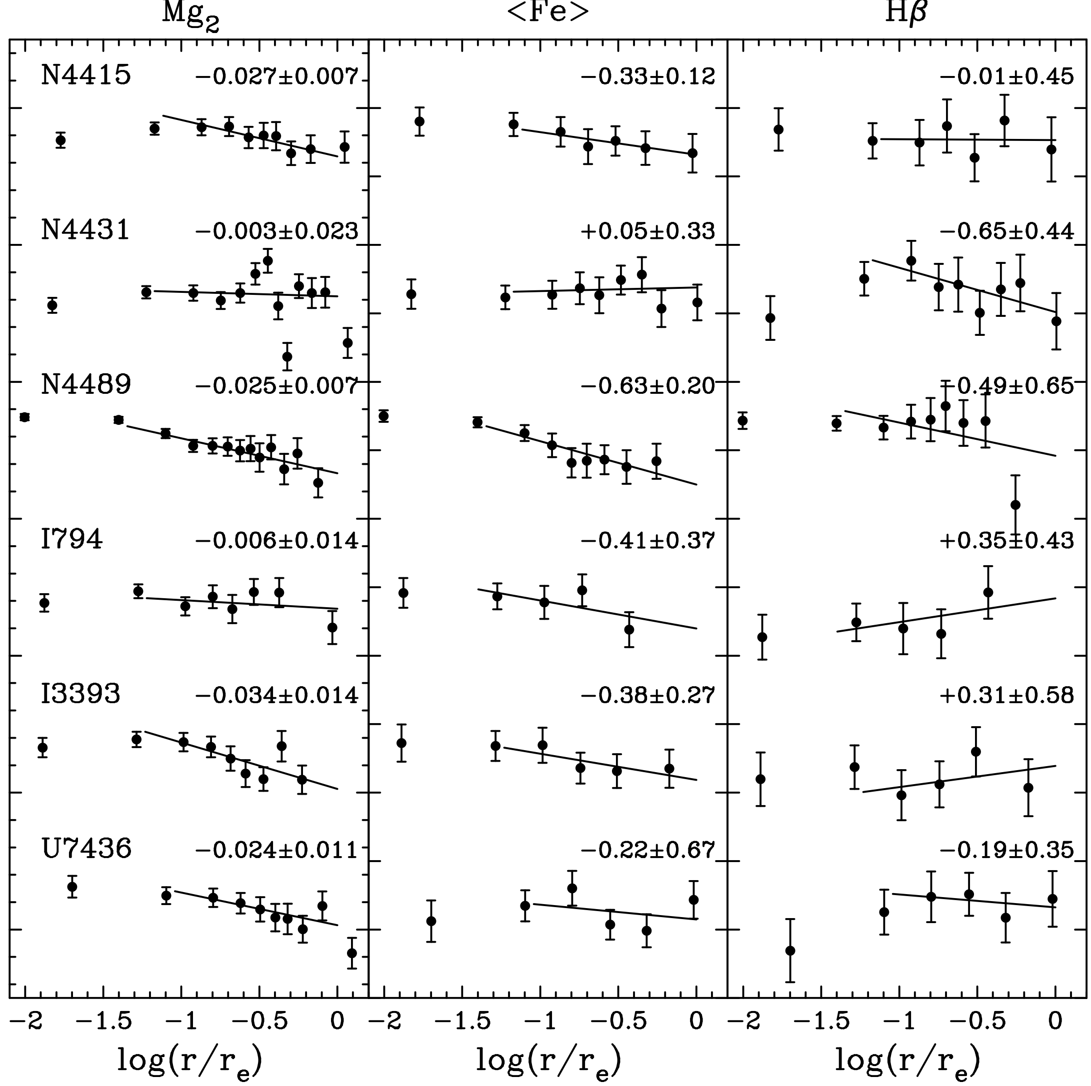

Mg2
<Fe>
Hβ
N4415
−0.027±0.007
−0.33±0.12
−0.01±0.45
N4431
−0.003±0.023
+0.05±0.33
−0.65±0.44
N4489
−0.025±0.007
−0.63±0.20
+0.49±0.65
I794
−0.006±0.014
−0.41±0.37
+0.35±0.43
I3393
−0.034±0.014
−0.38±0.27
+0.31±0.58
U7436
−0.024±0.011
−0.22±0.67
−0.19±0.35
−2
−1.5
−1
−0.5
0
log(r/re)